Supplementary Information: Emergent dynamic chirality in a thermally driven artificial spin ratchet

Sebastian Gliga[1,2,3,*], Gino Hrkac[4], Claire Donnelly[2,3], Jonathan Büchi[2], Armin Kleibert[3], Jizhai Cui[2,3], Alan Farhan[2,3,5], Eugenie Kirk[2,3], Rajesh V. Chopdekar[6], Yusuke Masaki[7], Nicholas S. Bingham[2,3,8], Andreas Scholl[5], Robert L. Stamps[1], Laura J. Heyderman[2,3]

1 SUPA, School of Physics and Astronomy, University of Glasgow, Glasgow, G12 8QQ, United Kingdom.

2 Laboratory for Mesoscopic Systems, Department of Materials, ETH Zurich, 8093 Zurich, Switzerland.

3 Paul Scherrer Institut, 5232 Villigen PSI, Switzerland.

4 College of Engineering, Mathematics and Physical Sciences, University of Exeter, Exeter, EX4 4QF, United Kingdom.

5 Advanced Light Source, Lawrence Berkeley National Laboratory (LBNL), 1 Cyclotron Road, Berkeley, California 94720, USA.

6 Department of Materials Science and Engineering, University of California, Davis, Davis, CA 95616, USA.

7 Department of Physics, The University of Tokyo, Tokyo, 113-0033, Japan.

8 National Research Council Research Associate at the U.S. Naval Research Laboratory 4555 Overlook Ave., SW Washington, DC 20375.

[*] Email: sebastian.gliga@glasgow.ac.uk

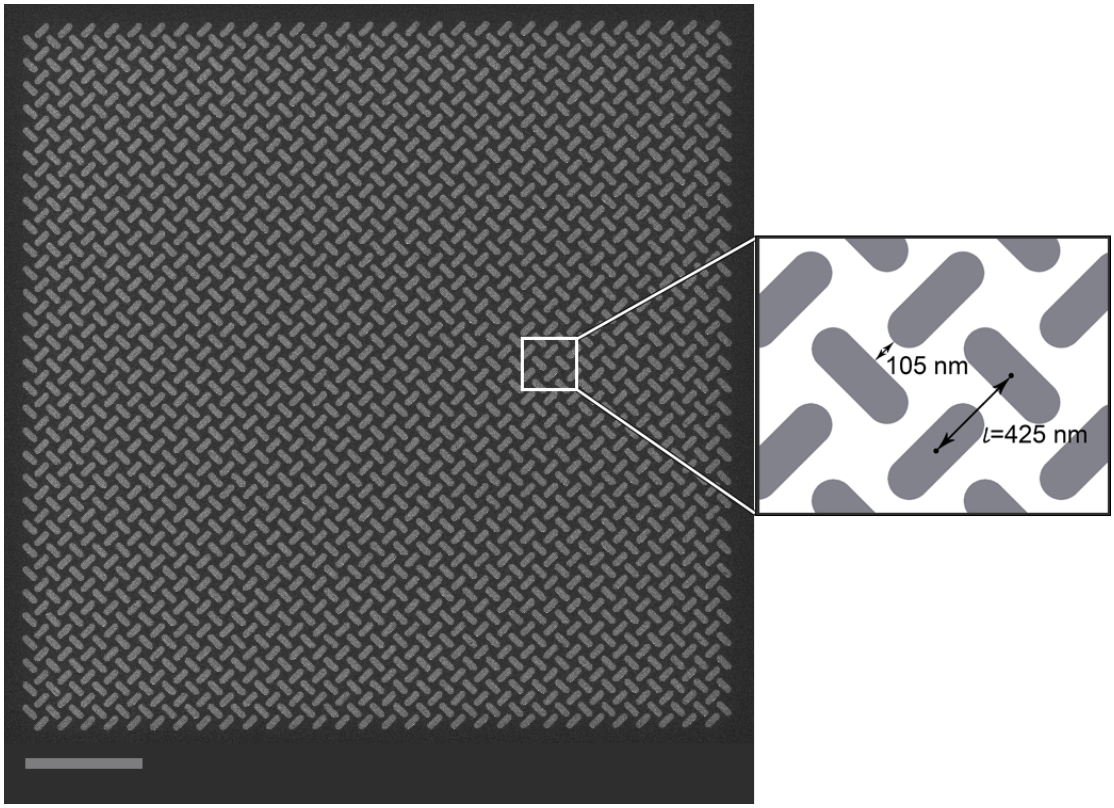

S1: SEM image of the experimentally studied array. The array is made of elongated Permalloy nanomagnets that are 470 nm long and 170 nm wide. The scale bar represents 3 μm. The inset indicates the centre-to-centre distance between nanomagnets (lattice constant, ι), which is 425 nm. The edge-to-edge nanomagnet separation is 105 nm.

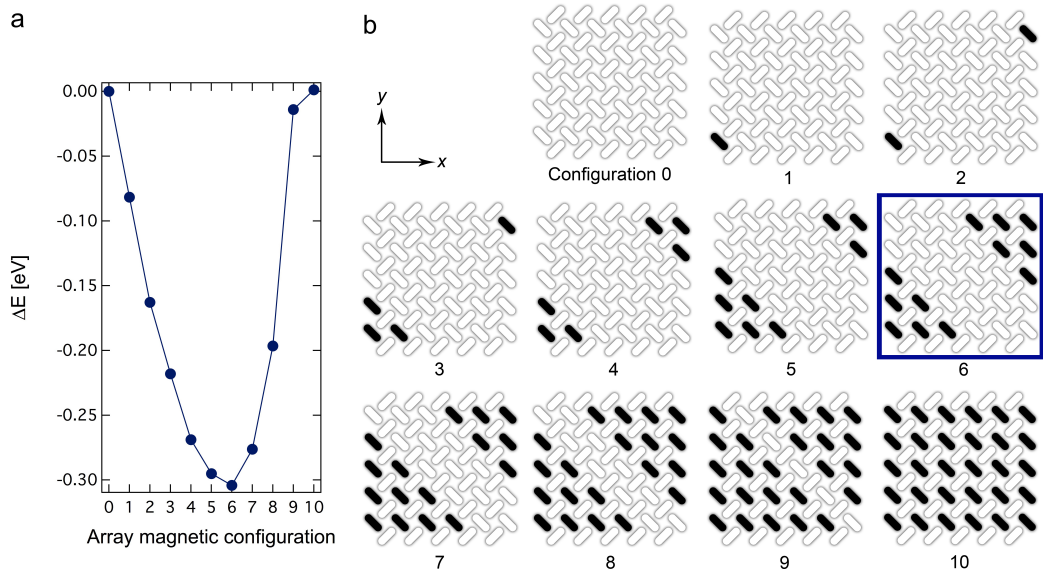

S2: Total energy of intermediate magnetic configurations during the evolution of the nanomagnet array from state A to state B. The total energies of different

magnetic configurations of the array in a system of 60 nanoislands with the same geometry as the experimental system, calculated in zero field using micromagnetic simulations (see Methods), are plotted in (a). The energies are relative to 'configuration 0' in (b) in which all vertices are in state A (see Figure 1 of the main text), following saturation. The white or black colours respectively indicate the direction of the magnetisation toward the positive or negative *y* axis. Configuration 6 in (b) (highlighted by the blue frame) is the minimum energy configuration, in which the magnetisation along six of the total ten diagonals has reversed, starting from two corners of the array, where the energy barrier to switching is lowest. (This configuration is consistent with the optimal distribution of the emergent surface 'charges', which are discussed in Figure 3.) Configurations 1-5 and 7-10 are examples of possible intermediate states, but are not part of a unique magnetisation reversal sequence for the evolution of the magnetisation in the array from state A to state B. In configuration 10 the net magnetisation of the array is fully rotated by 90°. The calculated lowest energy configuration can be compared to the experimentally observed state in Figure 2d of the main text at t=4 hours, in which the magnetisation reversals mostly occur along diagonals starting from the same corners as in configuration 6. The differences are mainly due to the presence of a weak bias field, as described in the Methods, as well as to the fact that the system has not had the time to fully relax in the experiment (see also Supplementary Information S3).

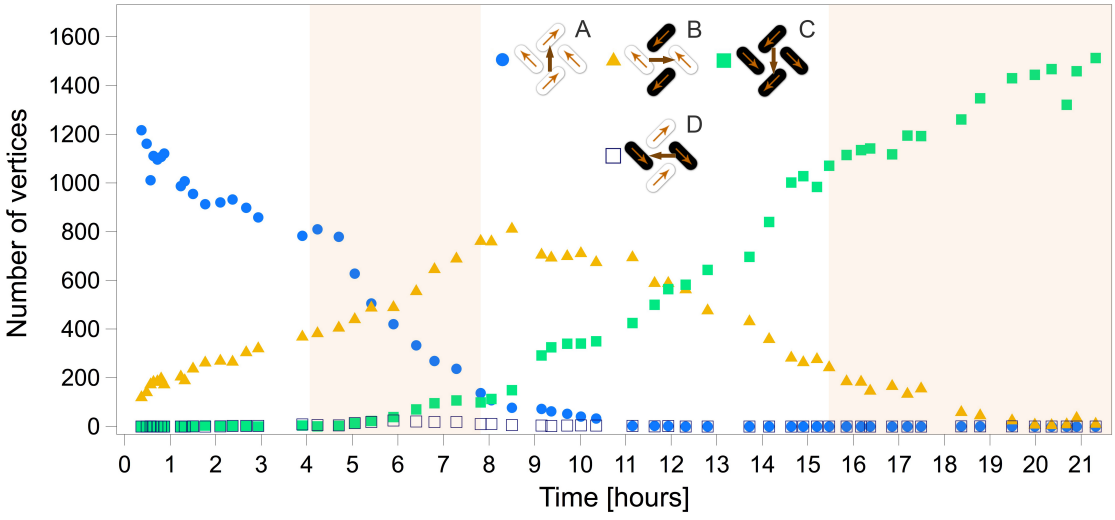

S3: Time-evolution of the different vertex states in the measurements shown in Figure 2 of the main text. The array has a total number of 1741 vertices; the starting number of vertices in state A (blue dots) is less than the total number of vertices, as imaging was performed 20 minutes after saturating the sample with a magnetic field, by which time the system had already started to relax. The shaded

regions represent the periods over which the sample was heated above room temperature.

At t=0, the saturating field defines an out-of-equilibrium state and the subsequent relaxation of the magnetisation at room temperature results in the decrease of the number of vertices in state A and an increase of vertices in state B. During the thermal evolution, the rotation of the net vertex magnetisation starts at the edges, as seen in Figure 2d of the main text (and later, in Figure 2f-g). After four hours the relaxation slows down and, in the absence of a bias field, the system would be expected to eventually reach an equilibrium state, corresponding to a minimum in the energy landscape (see configuration 6 in Supplementary Information S2). However, we observe that the rotation of the average vertex magnetisation continues once the sample temperature is increased by about 5K (first shaded region, between t=4 and t=8 hours), as seen by the increase in the number of vertices in configuration B, and the almost vanishing number of vertices in state A at t=8 hours. We attribute this evolution to the presence of the bias field (shown in Figure 2 of the main text), indicating that the field modifies the energy landscape of the system to further the clockwise rotation of the average magnetisation. After approximately 15 hours, heating by about 7K (second shaded region starting at t=15.5 hours) helps the system evolve into an almost fully saturated state, in which the average vertex magnetisation was rotated by 180° with respect to the initial state (state C).

The number of vertices in state D is also plotted for reference, showing that this state is not accessed during the thermal evolution, quantitatively demonstrating the ratchet behaviour.

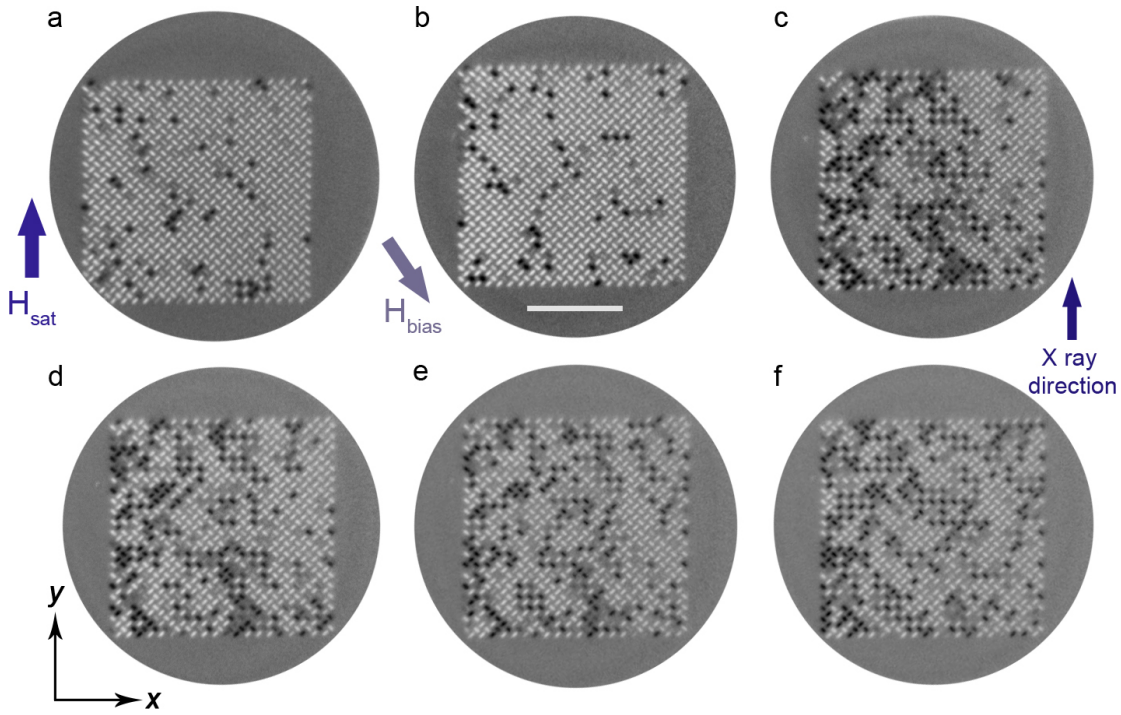

S4: Absence of chiral dynamics due to reduced magnetostatic coupling in a system with larger edge-to-edge separation between individual nanomagnets. The measured thermal relaxation at room temperature covers a period of 4.5 hours in a system in which the thermally active nanomagnets have a lateral size, which is 60% of the ones in Figure S1 (and in Figure 2 of the main text), while keeping the same lattice constant of 425 nm. This effectively increases the edge-to-edge distance between the islands to 233 nm and reduces the magnetic volume, such that the strength of the magnetostatic coupling is reduced. The array edge geometry is the same as in Figure S1. The scalebar represents 5 μm. The system is initially saturated by an external field, $\boldsymbol{H}_{sat}$, in the *+y* direction. The bias field ($\boldsymbol{H}_{bias}$) is the same as in Figure 2 of the main text. The XMCD images are taken following saturation at a) 0.5 hour b) 1 hour c) 2.5 hours d) 3 hours e) 4 hours and f) 4.5 hours. In this case, we do not observe an overall chiral evolution of the magnetisation, confirming that the magnetostatic coupling is responsible for the measured dynamic chirality (Figure S3).